

Optical and structural characteristics of ZnO nanopowders for different preparation methods

Glécia V. S. Luz^{1,2*}, Emerson R. Santos¹, Leandro X. Cardoso², Lourdes M. Brasil², Pilar Hidalgo^{2*}, Wang S. Hui¹

¹Departamento de Metalurgia e Materiais, Escola Politécnica da USP, Universidade de São Paulo-USP, Av. Prof. Mello Moraes 2463, São Paulo-SP, 05508-030, Brazil

²UnB Gama-FGA, Universidade de Brasília-UnB, Área Especial de Indústria Projeção A, Brasília-DF, 72444-240, Brazil

*Corresponding authors: Tel: (+55) 61998672027, (+55) 6130410715; E-mail: gleciavs@gmail.com, drapilar@gmail.com

Received: 29 December 2016, Revised: 15 February 2017 and Accepted: 09 April 2017

DOI: 10.5185/amlett.2017.1581

www.vbripress.com/aml

Abstract

Zinc oxide (ZnO) nanoparticles (NPs) were synthesized by different methods known as Pechini and Sol-Gel. It was observed during the experiments significant differences comparing these methods as: particle size, time applied, crystallinity and chemical residues generated by-products. The NPs were analysed by X-ray diffraction (XRD), ultraviolet-visible (UV-Vis.) absorption and Raman spectroscopy techniques. X-Ray Diffractograms showed peaks corresponding to hexagonal wurtzite crystalline structure. It was observed that NPs obtained by the Pechini showed better homogeneity and crystallinity; these presented average size of 115 nm. The NPs produced by Sol-Gel method showed crystallites with smaller average size of 8 nm. The band gap energy (E_g) obtained using UV-Vis for ZnO NPs synthesized by Pechini was 3.39 eV. Still, the results for Sol-Gel method with 5 and 10 hours of reactions were 3.53 eV and 3.55 eV respectively. Raman data obtained by Pechini and Sol-Gel Methods showed characteristics peaks. The obtained data confirmed the ZnO phase samples and the proportional relationship to the enlargement with the intensity of peaks $E_{2\text{ High}} - 438\text{ cm}^{-1}$, as evidenced by literature. These results lead to the applicability of both NPs in optoelectronic and fluorescent applications. Copyright © 2017 VBRI Press.

Keywords: ZnO, nanoparticles, pechini method, sol-gel method.

Introduction

Zinc oxide (ZnO) is an inorganic semiconductor compound extensively used in several materials and products including: plastic, ceramic, glass, cement, rubber, lubricant and photo-electrovoltaic devices including also the medical area [1–13]. For this reason, there is a great demand for new information for scrutiny about this material formed from synthesis methods and analyzed through its optical, electrical and morphological characteristics. ZnO can crystallize in hexagonal wurtzite, cubic zinc blend or cubic rock salt. It is also n-type semiconductor that absorbs UV light and presents transparency in the visible light [14–17]. ZnO nanoparticles (NPs) often have a tendency to grow along the c-axis of the wurtzite crystal. New methods of synthesis could lead to obtaining ZnO NPs with different grain sizes. In the preparation of ZnO some techniques are included as: Pechini [1–6], wet chemical [7], Sol-Gel [18–23], electroplating [24–27], sonochemical [28], hydrothermal [29–31], zinc-air system [32] and spray pyrolysis [33].

The **Table 1** shows some papers published in recent years, their synthesis techniques and the size of the smallest nanoparticles found. An intent analysis comparing different techniques contributed to the choice of the better methods to obtain smaller NPs. Moreover,

other characteristics were also analyzed, as: homogeneity, materials involved with inexpensive reagents, good optical characteristic, low temperature and easy process control.

Table 1. Some papers of ZnO NPs found in the literature with: methods used, grain sizes and homogeneity obtained [34–41].

Authors	Method	Average size of ZnO NPs ^[a] (nm)	Homogeneity of NPs
Poul et al. (2001)[34]	Poliol	340	Yes
Wang et al. (2005)[35]	Forced hydrolysis	~500	Yes
Choi et al. (2005)[36]	Sol-Gel	25±1.5	Yes
Luyuan et al. (2010)[37]	Sol-Gel	2.2-7.8	Yes
Alias et al. (2014)[38]	SGS ^[b]	330-530	No
Alias et al. (2014)[38]	SGC ^[c]	20-80	Yes
Barros et al. (2006)[39]	Pechini ^[d]	24-55	Yes
He et al. (2008)[40]	Pechini ^[d]	25-82	Yes
Rautio et al. (2009)[41]	Pechini ^[d]	16-76	Yes

[a] NPs = Nanoparticles. [b] SGS = Sol-Gel Synthesis for storage. [c] SGC = Synthesis with Sol-Gel centrifugation. [d] For different temperatures of calcination.

Two methods of synthesis were selected in this work, namely, Pechini and Sol-Gel Methods. The ZnO NPs obtained were analyzed with special attention given to the optical and structural characterization.

Experimental

Materials

The polyester formed via Pechini method [5] used zinc nitrate ($\text{ZnC}_6\text{H}_6\text{O}_7 \cdot \text{H}_2\text{O}$), ethylene glycol monohydrate P.A. (EG) ($\text{C}_2\text{H}_6\text{O}_2 \cdot \text{H}_2\text{O}$), ethyl alcohol P.A. (CH_3CHOH), citric acid (CA) monohydrate ($\text{C}_6\text{H}_8\text{O}_7 \cdot \text{H}_2\text{O}$) purchased from Vetec Company.

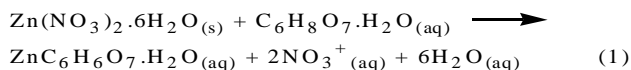
The Sol-Gel method used four types of materials for synthesis of the ZnO NPs: precursor, solvents, catalyst and stabilizer. These reagents were: zinc chloride (P.A.) (ZnCl_2) purchased from ACS-Impex, sodium oleate ($\text{C}_{18}\text{H}_{33}\text{O}_2\text{Na}$) $\geq 82\%$ fatty acids purchased from Sigma-Aldrich, ethyl alcohol (P.A.) (CH_3CHOH), $\text{LiOH} \cdot \text{H}_2\text{O}$ and hexane (P.A.) (C_6H_{14}) from Vetec Company and distilled water.

Synthesis of ZnO nanoparticles by Pechini Method

The polyester is formed by balanced chemical reaction, then the solution is heated at from 180 °C to 220°C and finally the precursor formed is calcined at 500°C to obtain a residual powder [2–4]. The proportion of Ethylene Glycol (EG) and Citric Acid (CA) influences the formation of nanoparticles, which is justified by the theory of collisions and Le Chatelier's Principle. However, according to the researches the calcination temperature is the factor that mostly affects the size of the crystallites [39,41]. Thus, the product is generated by higher concentration of ethylene glycol with higher frequency and collision between the reactants.

The experimental procedures (based in the work of Razavi *et al.* (2012) [5], are described by different steps:

1) Chelate-forming cations (Zn^{2+}): The zinc nitrate ($\text{ZnC}_6\text{H}_6\text{O}_7 \cdot \text{H}_2\text{O}$) was solubilized in deionized water. After added citric acid monohydrate ($\text{C}_6\text{H}_8\text{O}_7 \cdot \text{H}_2\text{O}$). See **Equation 1**:



2) Polymerization reaction (or polyesterification): the mixture of zinc nitrate and citric acid was added containing ethylene monohydrate ($\text{C}_2\text{H}_6\text{O}_2 \cdot \text{H}_2\text{O}$) P.A. at 52 °C. The solution was stirred and heated for 1 hour. See **Equation 2**.

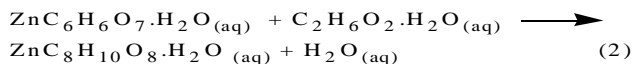


Table 2. Steps of solution heating to obtain ZnO nanoparticles.

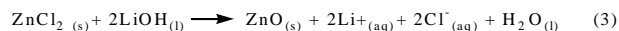
Initial Temperature (°C)	Rate (°/min.)	Time (min.)	Finish Temperature (°C)
30	10	8	80
80	0	60	80
80	10	7	150
150	0	60	150
150	10	60	600
600	0	60	600
600	-3.17	180	30

3) Formation of ZnO: After the polymerization reaction, the solution was heated in an automatic muffle following heating ramps to eliminate the organic component and moisture. Thus, the synthesis was started dissolving the cationic component (5.00 ± 0.01 g), which in this case is zinc nitrate, in H_2O deionized (15.00 ± 0.03 mL). After added citric acid monohydrate (5.02 ± 0.01 g).

Then the mixture of zinc nitrate and CA was added into a beaker containing EG at 52°C. The proportion of EG and CA used was 2:1. This solution was stirred and heated for 1 hour, following the temperature ramps described in **Table 2** to eliminate the organic component and moisture.

Synthesis of ZnO Nanoparticles by Sol-Gel Method

In the Sol-Gel method, four types of materials were used to perform of ZnO NPs synthesis, as: precursor, solvents (ethanol mixed with hexane and distilled water), catalyst and stabilizer. The reaction occurs by steps: hydrolysis, condensation and polymerization of monomers to form particles, particle growth and finally, particle agglomeration. In the reaction process, the particle nucleation occurs by precipitation according to the following equation (**Equation 3**) [1,42]:



The process of crystal growth takes place in a supersaturated solution to achieve a good chemical balance by the solid solution saturation. After the growth step, the average particle size and mean distribution can be modified by aging process, which is primarily the aggregation and coarsening, which are directly dependent of experimental parameters, as: time, precursor and temperature of reaction.

This work was carried out without the use of high temperatures [1,20]. Thus, the synthesis was divided in four parts, adapted from the method used for Choi *et al.* [36] and Zhang *et al.* [37]:

- 1) Zinc chloride (ZnCl_2) (5.45 ± 0.01 g (40 mmol)) and sodium oleate ($\text{C}_{18}\text{H}_{33}\text{O}_2\text{Na}$) (24.35 ± 0.01 g (80 mmol)) were dissolved in a solvent mixture consisting of ethanol (80.00 ± 0.10 mL), distilled water (60.00 ± 0.10 mL) and hexane (140.00 ± 0.10 mL). The solution was refluxed for 4 h at 70.00 ± 0.01 °C. Initially the solution turns into yellow opaque, moving to the formation of two phases;
- 2) After four hours of reaction, the upper organic layer containing zinc oleate complex ($\text{C}_{36}\text{H}_{33}\text{O}_4\text{Zn}$) was washed by three times with distilled water (30.00 ± 0.05 mL) in a separator funnel. After evaporation of the hexane only zinc oleate complex (ZO) remained in the funnel;
- 3) Subsequent to obtaining ZnO were added this complex (6.28 ± 0.01 g) and ethanol (100.00 ± 0.10 mL) were added into a flask equipped with condenser. Then the system was heated to 70°C and ZnO complex was dissolved under constant magnetic stirring;

- 4) Molar ratio of $Zn^{2+}/LiOH$, $LiOH.H_2O$ was dissolved in ethanol (100.00 ± 0.10 mL) with the aid of ultrasonic radiation and the obtained solution was added to the ZnO solution prepared previously. The estimated time of reaction was 5 hours. To obtain the purest ZnO nanoparticles, the crystals were washed with portions of hexane and ethanol.

Characterizations

ZnO nanoparticles were characterized by XRD patterns recorded on a Bruker D8-Discover diffractometer, with Cu $K\alpha$ radiation. The angle (2θ) range was from 25° to 90° in a continuous scan of $0.020^\circ/\text{min}$. Rietveld analysis measurements were performed using scan step mode with 2θ varying from 25.00° to 89.98° with $0.020^\circ/\text{min}$ of scanning velocity. UV-Vis. for the optical absorbance was collected with a spectrophotometer, model Evolution 220 of Thermo Scientific. The Raman effect in ZnO was measured using the Horiba HR800, with laser at 784 nm as excitation source. All measurements in this work were carried out at room temperature.

Results and discussion

XRD analyses

The **Fig. 1** shows the XRD patterns of ZnO nanopowders obtained by Pechini and Sol-Gel methods. All diffraction peaks can be indexed as a wurtzite crystalline structure, but the spectrum of the "ZnO Sol-Gel 10h" showed an extra peak, possibly of contaminant by time of sample storage. The results were based on the hexagonal tetragonal space group $P6_3mc$ (code 186), with lattice parameters $a=b=3.81 \text{ \AA}$ and $c=6.23 \text{ \AA}$ and internal coordinates Zn (0.6667; 0.3333; 0.0) and O (0.6667; 0.3333; 0.375) [43, 44], in agreement with the Joint Committee on Powder Diffraction Standards (JCPDS) card 36-1451. These results indicate that the nanopowders by both syntheses are free of other phases. Using the methodology that allows the refinement of complex crystal structures, which is known as Rietveld method, provided a diffractogram calculated from the information of the crystal structures of phases present and their relative proportions. The procedure sets the actual and calculated diffractograms with minimization of residue by minimum square [45, 46]. It is possible to calculate the average size of crystallites analyzed and, in this case, the crystallite size may be obtained by measuring the Bragg peak width at half the maximum intensity and using also the Debye-Scherrer law [47] (**Equation 4**):

$$D = \frac{0.916 \times \lambda}{\beta \times \cos \theta} \quad (4)$$

where D is the crystallite size, λ is the wavelength of the X-radiation used in the analysis, β is the Bragg peak width at half the maximum intensity and θ is the Bragg angle [48]. **Equation 5** was used for the calculations of wavelength (λ) set to Lorentzian calculations:

$$M_L = M_{HW} - 0.15 \quad (5)$$

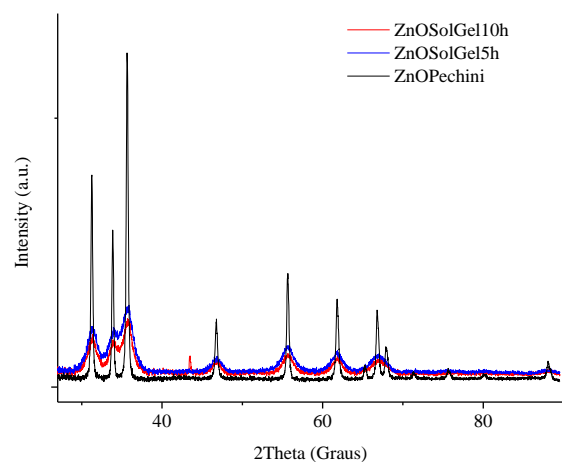


Fig. 1. X-ray diffractograms of ZnO nanoparticles, synthesized with Pechini and Sol-Gel methods (by 5 and 10 hours of reaction).

Thus, for this study, D was calculated by **Equation 6**:

$$D = \frac{0.916 \times 15.42 \times 10^{-11}}{M_L \times \frac{\pi}{180} \times \cos \theta \times \frac{\pi}{360}} \quad (6)$$

The average diameters of crystallite were estimated by the most intense peak (101). The size of the ZnO NPs is modified according to the method of synthesis and reaction time (for Sol-Gel method), as expected. The average crystallite size for the Pechini Method was 115.2 nm. The average size for the ZnO NPs obtained by Sol-Gel method was 7.6 and 8.3 nm for 5 and 10 hours of reaction, respectively.

Rietveld refinements analyses of all samples ZnO are shown in **Fig. 2**. The patterns were calculated with a series of structural parameters, as: cell, atomic coordinates, peak shape and width parameters

Table 3. Some papers of ZnO NPs found in the literature with: methods used, grain sizes and homogeneity obtained Crystal data and refinement factors of ZnO NPs obtained from XRD data.

ZnO NPs Samples	Unit cell parameters (Å)		α (°)	β (°)	γ (°)	Space group	Volume (Å ³)	D-Scherrer (nm)
	a=b	c						
ZnO Pattern[44]	3.253	5.207	-	-	-	$P6_3mc$	-	-
ZnO Pechini	3.296	5.280	90	90	120	$P6_3mc$	49.685	115.23
ZnO Sol-Gel 5h	3.307	5.292	90	90	120	$P6_3mc$	50.133	7.55
ZnO Sol-Gel 10h	3.305	5.290	90	90	120	$P6_3mc$	50.024	8.27

(background, Lorentz-polarization correction), comparing the data obtained [45,46]. The Figure shows the statistical results between the pattern $P6_3mc - 186$ (Cal. = the theoretical data.) and the spectra obtained (Obs. = the experimental data), too the Bragg Position that indicate the peak position for each syntheses. The Different statistical agreement factors between data (Dif., R_p , R_{wp} and R_{exp}) are presented. The R_{wp} factor so called weighted profile, the R_p (patterns factor) and R_{exp} (expected weighted profile factor) measure not just how well the structural model fits the experimental diffraction intensities, but also the fit of the background, the diffraction positions and peak shapes [49,50].

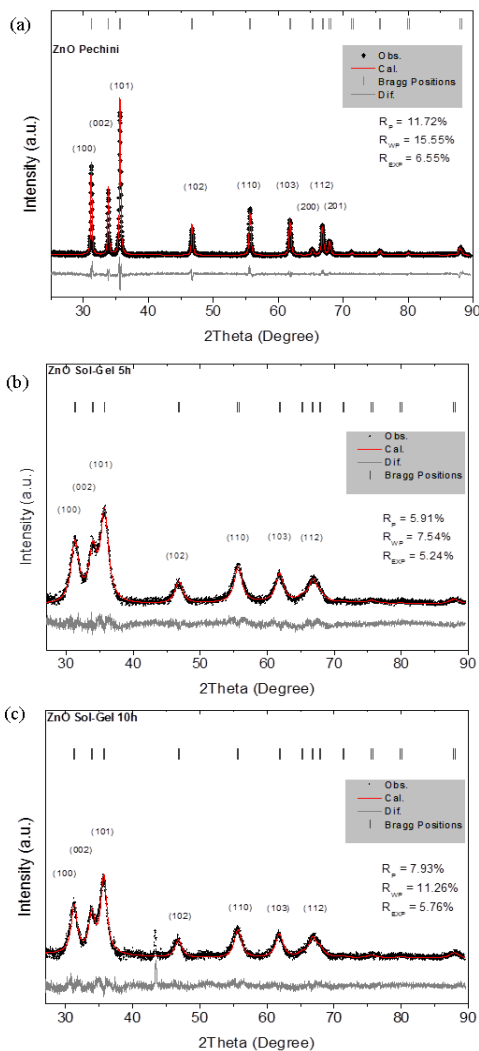


Fig. 2. XRD patterns refined with Rietveld method of ZnO nanoparticles synthesized by: (a) Pechini Method. (b) Sol-Gel Method with 5 hours of reaction. (c) Sol-Gel with 10 hours of reaction.

It can be seen in **Fig. 2** that the profiles observed and calculated are perfectly matching, except for a peak at approximately 44° for the sample "ZnO Sol-Gel - 10h", possibly associated to a second contaminant phase. This point increased the value of R_{wp} of this sample compared with the sample "ZnO Sol-Gel - 5h". In general terms, R-factors values may be considered very good for estimations. The methods of synthesis were satisfactory to obtain the nanoparticles with a hexagonal unit cell, with

crystal quality and purity, especially in samples "ZnO Pechini" and "ZnO Sol-Gel - 5h". The crystal results and refinement factors of ZnO NPs obtained from XRD data are shown in **Table 3**.

The lattice parameters as obtained for ZnO NPs are in agreement with the report of literature (JCPDS:89-0510) [44] and the volume is proportional to the unit cell parameters obtained. The value of lattice strain may be due to the procedure adopted in the synthesis of nanoparticles, like temperature and quantity of reagents used.

UV-Vis. absorption and band gap energy (E_g)

In the **Fig. 3** the Spectra UV-Vis of the ZnO NPs obtained is showed. Characteristic wavelengths were noted observed. The samples had a broad absorption in the range from 200 to 460 nm. The sample value of the wavelength associated with the transition ZnO NPs (valence band (VB) - conduction band (CB)) were observed by methods: Pechini = 366 nm; Sol-Gel (5 hours of reaction) = 349 nm and Sol-Gel method (10 hours of reaction) = 351 nm.

All absorbance values were shown to be consistent with those observed in the literature. It is important to note that the energy of the nanoparticle will decrease the larger the radius of the particle and the light absorption is shifted: ZnOSolGel - 5h < ZnOSolGel - 10h < ZnOPechini.

The band gap energy (E_g) is a factor of great importance for characterization of insulator and semiconductor materials. Burger [51] relates that this energy can be characterized by various methods.

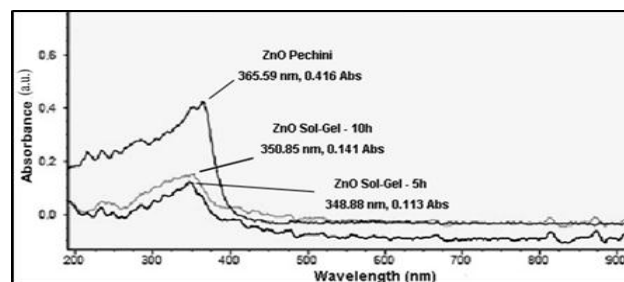


Fig. 3. UV-Vis. spectra for samples of ZnO obtained by Pechini and Sol-Gel Method (at 5 and 10 hours of reaction).

One method is the spectroscopy of Diffuse Reflectance Technique (DRS) in the UV-Vis. that is influenced by type of sample, powder or film and parameters, as: thickness and size of the crystals. The Kubelka and Munk model [52] is widely used for this type of study. The model is based on the assumption that the diffuse reflectance arises from the absorption and scattering of light by a surface. For example, in the work of Wang [53], the E_g value found was 3.37 eV. Nevertheless Feltrin [54] obtained a value of 3.18 eV. This study also used the assumption according to **Equation 7**, which was modeled on Kubelka and Munk:

$$E_g = h\nu_g = h \frac{c}{\lambda_g} = \frac{1240}{\lambda_g} \quad (7)$$

Where $h = 6.63 \times 10^{-34}$ J.s (Planck constant), $\nu_g =$ Transition Frequency VB→CB and, c is the speed of light in vacuum ($\approx 3 \times 10^8$ m/s). The E_g values obtained for the synthesized ZnO are consistent with literature. It reports for semiconductors a variation of energy from 0.2 to 4.0 eV [55]. The values obtained possibly contribute to increase the transfer rate of charge carrier. The higher bandgap, is the lower wavelength of light absorbed and/or emitted, that in this experiment revealed to be the "ZnO Pechini" sample.

Raman spectroscopy analysis

In the Raman spectroscopy analysis the active zone-center optical phonons predicted by the group theory (C_{4v}^2) are $A_1+2E_2+E_1$. The phonons symmetry and polar phonons are A_1 and E_1 with different frequencies for the transverse optical (TO) and longitudinal optical (LO) phonons. In semiconductor ZnO NPs, the non-polar phonon modes with symmetry are E_2 (high) associated with oxygen atoms and E_2 (low) that is associated with Zn sublattice [56,58–60]. Fig. 4 shows the results of the calculations for ZnO NPs by three samples, where it can see the non-polar optical phonon.

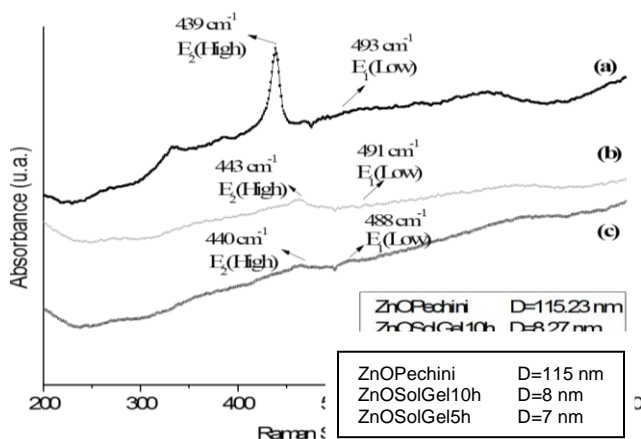


Fig. 4. Raman spectra of ZnO nanoparticles under 784 nm excitation. The results are obtained by backscattering configuration. (a) ZnO Pechini, (b) ZnO SolGel 10 h and (c) ZnO Sol Gel 5 h.

Table 4. Raman active phonon mode frequencies (in cm^{-1}) for ZnO NPs samples comparing with the literature (nd.=not detectable).

ZnO NPs Samples	$A_1(\text{TO})$	$E_1(\text{TO})$	$E_2(\text{High})$	$A_1(\text{LO})$	$E_1(\text{Low})$
ZnO[56]	381	407	437	574	583
ZnO[57]	379	410	437	577	592
ZnO Pechini	385	401	438	469	493
ZnO Sol-Gel 5h	387	nd.	440	468	488
ZnO Sol-Gel 10h	384	nd.	443	463	491

Table 4 and Fig. 4 showed the results of the calculations for ZnO NPs samples compared to results of literature. The ZnO mode for the E_2 and E_1 vibrations could be easily identified. The results confirm the existence of the ZnO phase samples and show in the intensity of $E_2(\text{High})$ peaks a proportional relationship to

the enlargement of the peaks and the diameter of the nanostructure, as also evidenced by literature [58].

Conclusions

The ZnO nanoparticles free of secondary phases and with hexagonal structure were synthesized by two different methods known as Pechini and Sol-Gel. The X-ray analysis showed a good crystallinity. Refinement analysis led to noticing that the Pechini method produced crystallites from 50 to 163 nm and the average of diameter was 115 nm. This result was obtained by slightly larger particles than expected, according to literature. For samples produced by the Sol-Gel method with 5 and 10 hours of reaction time, the edge of the crystallite sizes were 8 nm and 7-9 nm and the average diameter were 7.6 and 8.3 nm, respectively.

The average size of the crystallites for the Pechini method was 93% greater than the average of the particles synthesized by the Sol-Gel method. It was also observed also a greater homogeneity in the size of the samples synthesized by Pechini method compared to Sol gel method. The band gap Energy obtained for ZnO NPs in Pechini method was obtained by 3.39 eV, while for the Sol-Gel method were respectively 3.55 and 3.53 eV to 5 and 10 hours of reaction, respectively.

However, improved characteristics as semiconducting and less complexity in processes, as the use of solvents and shorter time of synthesis were obtained with the Pechini method, that it can be considered as better option for reaction known as "chemical green", which reduces the residues launched on the nature, but the correct choice will be evaluated depending of objective proposed by researcher, because, particle size, homogeneity, optical property and generation of waste are considerably different for both processes. The results have confirmed the applicability of both nanoparticles in optoelectronic and fluorescent applications, making this material a promising potential for investigations already under study by several researchers.

Acknowledgements

The authors would like to thank to CAPES-MEC Government of Brazil for the Pos-doctoral scholarship to Dr. Glécia V. da S. Luz, and Macromolecules Laboratory of the Polytechnic School, São Paulo University. To CNPq National Council for Scientific and Technological - Brazil Process No 555778/2010-0 and 408108/2013-4 for financial support into The Laboratory of Nanotechnology/FGA-UnB. Besides to the Laboratory of Magnetic Nanostructures/IF-UnB, and to the Laboratory of National Institute of Criminology/Federal Police for the technical support.

References

- Pechini, M. P.; Method of Preparing Lead and Alkaline Earth Titanates and Niobates and Coating Method Using the Same To Form a Capacitor, US3330697, 1967.
- Pereira, G. J.; Castro, R. H. R.; Hidalgo, P.; Gouvêa, D.; *Appl. Surf. Sci.*, **2002**, 195, 277. DOI: [10.1016/S0169-4332\(02\)00567-6](https://doi.org/10.1016/S0169-4332(02)00567-6)
- Castro, R. H.; Hidalgo, P.; Peres, H.; Fernandez, J. R.; Gouvêa, D.; *Sensors Actuators B Chem.*, **2008**, 133, 263. DOI: <http://dx.doi.org/10.1016/j.snb.2008.02.021>

4. Sakka, S.; Kozuka, H., Eds.; In *Handb. Sol-Gel Sci. Technol. Process. Charact. Appl.*; Kluwer Acad. Publish: Boston/Dordrecht/London: **2005**.
5. R.S. Razavi; Loghman-Estarkib, M. R.; Farhadi-Khouzani, M.; *Acta Phys. Pol. A*, **2012**, *121*, 98.
DOI: [10.1007/s11671-009-9401-z](https://doi.org/10.1007/s11671-009-9401-z)
6. Gonçalves, A. de S.; Lima, S. A. M. de; Davolos, M. R.; *Eclética Química*, **2002**, *27*, 293.
DOI: <http://dx.doi.org/10.1590/S0100-46702002000200025>
7. Das, N. C.; Sokol, P. E.; *Renew. Energy*, **2010**, *35*, 2683.
DOI: [10.1016/j.renene.2010.04.014](https://doi.org/10.1016/j.renene.2010.04.014)
8. Al-saadi, T. M.; Bakr, N. A.; Hameed, N. A.; *Int. J. Eng. Tech. Res.*, **2014**, *2*, 191.
9. Li, J.; Sang, X.; Chen, W.; Qin, C.; Wang, S.; Su, Z.; Wang, E.; *Eur. J. Inorg. Chem.*, **2013**, 1951.
DOI: [10.1002/ejic.201201120](https://doi.org/10.1002/ejic.201201120)
10. Chen, C. K.; Shen, Y.-P.; Chen, H. M.; Chen, C.-J.; Chan, T.-S.; Lee, J.-F.; Liu, R.-S.; *Eur. J. Inorg. Chem.*, **2014**, *2014*, 773.
DOI: [10.1002/ejic.201301310](https://doi.org/10.1002/ejic.201301310)
11. Dutta, R. K.; Sharma, P. K.; Pandey, A. C.; *Adv. Mater. Lett.*, **2011**, *2*, 268.
DOI: [10.5185/amlett.indias.195](https://doi.org/10.5185/amlett.indias.195)
12. N. Sharma, G.; Dutta, S.; Chatterjee, R.; Kumar Singh, S.; *Adv. Mater. Lett.*, **2016**, *7*, 951.
DOI: [10.5185/amlett.2016.6509](https://doi.org/10.5185/amlett.2016.6509)
13. Sivalingam, Y.; Magna, G.; Pomarico, G.; Martinelli, E.; Paolesse, R.; D'Amico, A.; Di Natale, C.; *Adv. Mater. Lett.*, **2012**, *3*, 442.
DOI: [10.5185/amlett.2012.icnano.144](https://doi.org/10.5185/amlett.2012.icnano.144)
14. Khan, A.; Synthesis, Characterization and Luminescence Properties of Zinc Oxide Nanostructures, Faculty of the College of Arts and Sciences, **2006**.
15. Grätzel, M.; *J. Photochem. Photobiol. C Photochem. Rev.*, **2003**, *4*, 145. DOI: [10.1016/S1389-5567\(03\)00026-1](https://doi.org/10.1016/S1389-5567(03)00026-1)
16. Beek, W. J. E.; Wienk, M. M.; Kemerink, M.; Yang, X.; Janssen, R. a J.; *J. Phys. Chem. B*, **2005**, *109*, 9505.
DOI: [10.1021/jp050745x](https://doi.org/10.1021/jp050745x)
17. Okazaki, K.; Kubo, K.; Shimogaki, T.; Nakamura, D.; Higashihata, M.; Okada, T.; *Adv. Mater. Lett.*, **2011**, *2*, 354.
DOI: [10.5185/amlett.2011.9093am2011](https://doi.org/10.5185/amlett.2011.9093am2011)
18. Meulenkamp, E. A.; *J. Phys. Chem. B*, **1998**, *102*, 5566.
DOI: [10.1021/jp980730h](https://doi.org/10.1021/jp980730h)
19. Hu, Z.; Oskam, G.; Penn, R. L.; Pesika, N.; Searson, P. C.; *J. Phys. Chem. B*, **2003**, *107*, 3124.
DOI: [10.1021/jp020580h](https://doi.org/10.1021/jp020580h)
20. Oskam, G.; *J. Sol-Gel Sci. Technol.*, **2006**, *37*, 161.
DOI: [10.1007/s10971-005-6621-2](https://doi.org/10.1007/s10971-005-6621-2)
21. Niederberger, M.; *Acc. Chem. Res.*, **2007**, *40*, 793. DOI:
22. Kwon, S. J.; Park, J.-H.; Park, J.-G.; *Appl. Phys. Lett.*, **2005**, *87*, 133112. DOI: [10.1063/1.2061871](https://doi.org/10.1063/1.2061871)
23. Kitsomboonloha, R.; Baruah, S.; Myint, M. T. Z.; Subramanian, V.; Dutta, J.; *J. Cryst. Growth*, **2009**, *311*, 2352.
DOI: [10.1016/j.jcrysgro.2009.02.028](https://doi.org/10.1016/j.jcrysgro.2009.02.028)
24. Leprince-Wang, Y.; Yacoubi-Ouslim, a.; Wang, G. Y.; *Microelectronics J.*, **2005**, *36*, 625.
DOI: [10.1016/j.mejo.2005.04.033](https://doi.org/10.1016/j.mejo.2005.04.033)
25. Tang, Y.; Luo, L.; Chen, Z.; Jiang, Y.; Li, B.; Jia, Z.; Xu, L.; *Electrochem. commun.*, **2007**, *9*, 289.
DOI: [10.1016/j.elecom.2006.09.026](https://doi.org/10.1016/j.elecom.2006.09.026)
26. Zeng, H.; Cui, J.; Cao, B.; Gibson, U.; Bando, Y.; Golberg, D.; *Sci. Adv. Mater.*, **2010**, *2*, 336.
DOI: <http://dx.doi.org/10.1166/sam.2010.1096>
27. Izaki, M.; Watanabe, M.; Aritomo, H.; Yamaguchi, I.; Asahina, S.; Shinagawa, T.; Chigane, M.; Inaba, M.; Tasaka, A.; *Cryst. Growth Des.*, **2008**, *8*, 1418. DOI: [10.1021/cg070164s](https://doi.org/10.1021/cg070164s)
28. Chen, Y. J.; Zhu, C. L.; Xiao, G.; *Sensors Actuators, B Chem.*, **2008**, *129*, 639.
DOI: [10.1016/j.snb.2007.09.010](https://doi.org/10.1016/j.snb.2007.09.010)
29. Guo, M.; Diao, P.; Wang, X.; Cai, S.; *J. Solid State Chem.*, **2005**, *178*, 3210.
DOI: [10.1016/j.jssc.2005.07.013](https://doi.org/10.1016/j.jssc.2005.07.013)
30. Sun, H.; Luo, M.; Weng, W.; Cheng, K.; Du, P.; Shen, G.; Han, G.; *Nanotechnology*, **2008**, *19*, 395602.
DOI: [10.1088/0957-4484/19/39/395602](https://doi.org/10.1088/0957-4484/19/39/395602)
31. Ma, T.; Guo, M.; Zhang, M.; Zhang, Y.; Wang, X.; *Nanotechnology*, **2007**, *18*, 35605.
DOI: [10.1088/0957-4484/18/3/035605](https://doi.org/10.1088/0957-4484/18/3/035605)
32. Yap, C. K.; Tan, W. C.; Alias, S. S.; Mohamad, A. A.; *J. Alloys Compd.*, **2009**, *484*, 934.
DOI: [10.1016/j.jallcom.2009.05.073](https://doi.org/10.1016/j.jallcom.2009.05.073)
33. Hosono, E.; Fujihara, S.; Honma, I.; Zhou, H.; *Adv. Mater.*, **2005**, *17*, 2091.
34. Poul, L.; Ammar, S.; Jouini, N.; Fiévet, F.; Villain, F.; *Solid State Sci.*, **2001**, *3*, 31.
DOI: [10.1016/S1293-2558\(00\)01129-8](https://doi.org/10.1016/S1293-2558(00)01129-8)
35. Wang, H.; Xie, C.; Zeng, D.; *J. Cryst. Growth*, **2005**, *277*, 372.
DOI: [10.1016/j.jcrysgro.2005.01.068](https://doi.org/10.1016/j.jcrysgro.2005.01.068)
36. Choi, S. H.; Kim, E. G.; Park, J.; An, K.; Lee, N.; Kim, S. C.; Hyeon, T.; *J. Phys. Chem. B*, **2005**, *109*, 14792.
DOI: [10.1021/jp052934i](https://doi.org/10.1021/jp052934i)
37. Zhang, L.; Yin, L.; Wang, C.; Lun, N.; Qi, Y.; Xiang, D.; *J. Phys. Chem. C*, **2010**, *114*, 9651.
DOI: [10.1021/jp101324a](https://doi.org/10.1021/jp101324a)
38. Alias, S. S.; Mohamad, A. A.; *Synthesis of Zinc Oxide by Sol-Gel Method for Photoelectrochemical Cells*; Springer: Singapore Heidelberg New York Dordrecht London, **2014**.
DOI: [10.1007/978-981-4560-77-1](https://doi.org/10.1007/978-981-4560-77-1)
39. Barros, B. S.; Barbosa, R.; Santos, N. R.; Barros, T. S.; Souza, M. a.; *Inorg. Mater.*, **2006**, *42*, 1348.
DOI: [10.1134/S0020168506120119](https://doi.org/10.1134/S0020168506120119)
40. He, G.; Cai, J. H.; Ni, G.; *Mater. Chem. Phys.*, **2008**, *110*, 110.
DOI: [10.1016/j.matchemphys.2008.01.023](https://doi.org/10.1016/j.matchemphys.2008.01.023)
41. Rautio, J.; Perämäki, P.; Honkamo, J.; Jantunen, H.; *Microchem. J.*, **2009**, *91*, 272. DOI: [10.1016/j.microc.2008.12.007](https://doi.org/10.1016/j.microc.2008.12.007)
42. Wong, E. M.; Hoertz, P. G.; Liang, C. J.; Shi, B.-M.; Meyer, G. J.; Searson, P. C.; *Langmuir*, **2001**, *17*, 8362.
DOI: [10.1021/la010944h](https://doi.org/10.1021/la010944h)
43. Lacerda, L. H. da S.; Lazaro, S. R. de; Ribeiro, R. A. P.; Oliveira, C. R. de; *An. do VII Work. Nanotecnologia Apl. ao Agronegócio*, **2013**, 425.
44. Kihara, K.; Donnay, G.; *Can. Mineral.*, **1985**, *23*, 647.
45. Rietveld, H. M.; *J. Appl. Crystallogr.*, **1969**, *2*, 65.
DOI: [10.1107/S0021889869006558](https://doi.org/10.1107/S0021889869006558)
46. Rietveld, H. M.; *Acta Crystallogr.*, **1967**, *22*, 151.
DOI: [10.1107/S0365110X67000234](https://doi.org/10.1107/S0365110X67000234)
47. Fenili, C. P.; Consolidação de aluminetos de ferro e níquel obtidos por moagem de alta energia, Universidade do Estado de Santa Catarina 2013, **2013**.
48. Suryanarayana, C.; *Prog. Mater. Sci.*, **2001**, *46*, 1.
DOI: [10.1016/S0079-6425\(99\)00010-9](https://doi.org/10.1016/S0079-6425(99)00010-9)
49. Dinnebier, R.; Friese, K.; In *Encycl. Life Support Syst.*; Ed.: P. Tropper(Eds.) Eolss Publishers: UK: **2003**.
50. Toby, B. H.; *Powder Diffr.*, **2006**, *21*, 67. DOI: [10.1154/1.2179804](https://doi.org/10.1154/1.2179804)
51. Bürger, T. S.; Desenvolvimento de Filmes de ZnO Para Aplicação Em Fotocatálise, Universidade Federal do Rio Grande do Sul, **2011**.
52. Murphy, A. B.; *J. Phys. D. Appl. Phys.*, **2006**, *39*, 3571.
DOI: [10.1088/0022-3727/39/16/008](https://doi.org/10.1088/0022-3727/39/16/008)
53. Wang, Z. L.; *J. Phys. Condens. Matter*, **2004**, *16*, R829.
DOI: [10.1088/0953-8984/16/25/R01](https://doi.org/10.1088/0953-8984/16/25/R01)
54. Feltrin, C. W.; Síntese E Propriedades Do ZnO: Correlação Entre Propriedades Estruturais E Atividade Fotocatalítica, Universidade Federal do Rio Grande do Sul, **2010**.
55. Atkins, P. w.; Shriver, D. F.; *Química Inorgânica - 4ª Ed.*; Bookman, **2008**.
56. Damen, T. C.; Porto, S. P. S.; Tell, B.; *Phys. Rev.*, **1966**, *142*, 570.
DOI: [10.1103/PhysRev.142.570](https://doi.org/10.1103/PhysRev.142.570)
57. Romcevic, N.; Kostic, R.; Romcevic, M.; Hadzic, B.; Kuryliszyn-Kudelska, I.; Dobrowolski, W.; Narkiewicz, U.; Sibera, D.; In *Proc. XXXVII Int. Sch. Semicond. Compd.*; ACTA PHYSICA POLONICA A: Jaszowiec: **2008**, pp. 1323-1328.
58. Kurtz, I. C.; Alim, K. A.; Fonoberov, V. A.; Krishnakumar, S.; Shamsa, M.; Balandin, A. A.; Russell; In *Proc. SPIE 6481-Quantum Dots, Part. Nanoclusters IV*; Eds.: K.G. Eyink, D.L. Huffake, F. Szmulowicz(Eds.) SPIE Proceedings: **2007**.
59. Alim, K. A.; Fonoberov, V. A.; Shamsa, M.; Balandin, A. A.; *J. Appl. Phys.*, **2005**, *97*, 124313.
DOI: [10.1063/1.1944222](https://doi.org/10.1063/1.1944222)
60. Ashkenov, N.; Mbenkum, B. N.; Bundesmann, C.; Riede, V.; Lorenz, M.; Spemann, D.; Kaidashev, E. M.; Kasic, A.; Schubert, M.; Grundmann, M.; Wagner, G.; Neumann, H.; Darakchieva, V.; Arwin, H.; Monemar, B.; *J. Appl. Phys.*, **2003**, *93*, 126.
DOI: [10.1063/1.1526935](https://doi.org/10.1063/1.1526935)